Deep-ultraviolet photonics for the disinfection of SARS-CoV-2 and its variants (Delta and Omicron) in the cryogenic environment

Wenyu Kang, Jing Zheng, Jiaxin Huang, Lina Jiang, Qingna Wang, Zhinan Guo, Jun Yin, Xianming Deng, Ye Wang and Junyong Kang

---

Related articles

Rapid inactivation of human respiratory RNA viruses by deep ultraviolet irradiation from light-emitting diodes on a high-temperature-annealed AlN/Sapphire template

Ke Jiang, Simeng Liang, Xiaojuan Sun, Jianwei Ben, Liang Qu, Shanli Zhang, Yang Chen, Yucheng Zheng, Ke Lan, Dabing Li, Ke Xu

Opto-Electronic Advances   2023 ,   doi: 10.29026/oea.2023.230004

More related article in Opto-Electron Journals Group website ↗

OEA | Opto-Electronic Advances

http://www.oejournal.org/oea

OE_Journal   @OptoElectronAdv

Deep-ultraviolet photonics for the disinfection of SARS-CoV-2 and its variants (Delta and Omicron) in the cryogenic environment

Wenyu Kang [1†*], Jing Zheng [2†], Jiaxin Huang [1], Lina Jiang [2], Qingna Wang [1,3], Zhinan Guo [2], Jun Yin [1*], Xianming Deng [4], Ye Wang [1] and Junyong Kang [1*]

Deep-ultraviolet (DUV) disinfection technology provides an expeditious and efficient way to suppress the transmission of coronavirus disease 2019 (COVID-19). However, the influences of viral variants (Delta and Omicron) and low temperatures on the DUV virucidal efficacy are still unknown. Here, we developed a reliable and uniform planar light source comprised of 275-nm light-emitting diodes (LEDs) to investigate the effects of these two unknown factors and delineated the principle behind different disinfection performances. We found the lethal effect of DUV at the same radiation dose was reduced by the cryogenic environment, and a negative-U large-relaxation model was used to explain the difference in view of the photoelectronic nature. The chances were higher in the cryogenic environment for the capture of excited electrons within active genetic molecules back to the initial photo-ionised positions. Additionally, the variant of Omicron required a significantly higher DUV dose to achieve the same virucidal efficacy, and this was thanks to the genetic and proteinic characteristics of the Omicron. The findings in this study are important for human society using DUV disinfection in cold conditions (e.g., the food cold chain logistics and the open air in winter), and the relevant DUV disinfection suggestion against COVID-19 is provided.

Keywords: LED; UV-C; III-nitrides semiconductors; photoelectronic; COVID-19; virucidal efficacy

Introduction

The coronavirus disease 2019 (COVID-19) pandemic is elicited by an RNA virus denominated severe respiratory syndrome coronavirus 2 (SARS-CoV-2)[1]. The spread of this virus and its variants, such as the Delta and Omicron, has negatively impacted the healthcare and economic systems global wide[2–5]. To reduce these negative effects, human beings have adopted methods of optics and photonics to identify or disinfect this virus effectively[6,7]. In particular, ultraviolet (UV) disinfection

[1]Engineering Research Center of Micro-nano Optoelectronic Materials and Devices, Ministry of Education, Fujian Key Laboratory of Semiconductor Materials and Applications, College of Chemistry and Chemical Engineering, Pen-Tung Sah Institute of Micro-Nano Science and Technology, College of Physical Science and Technology, Xiamen University, Xiamen 361005, China; [2]Xiamen Center for Disease Control and Prevention, Xiamen 361021, China; [3]Xiamen Intelligent Health Research Institute, Xiamen 361009, China; [4]School of Life Sciences, Xiamen University, Xiamen 361005, China.

[†]These authors contributed equally to this work.

*Correspondence: WY Kang, E-mail: wykang@xmu.edu.cn; J Yin, E-mail: jyin@xmu.edu.cn; JY Kang, E-mail: jykang@xmu.edu.cn

Received: 14 December 2022; Accepted: 22 March 2023; Published online: 9 June 2023

technology has received extensive attention for SARS-CoV-2 inactivation thanks to its great serviceability on the major media (bio-contaminated air and surfaces) for disease transmission[7–9].

UV light has been utilised for several decades to develop highly efficient and chemical-free technology to control microbial growth in many media[10]. As one of the microorganisms, viruses do not contain a nucleus but comprise either DNA or RNA within their protein coat. The deep-UV (DUV, wavelength ranging from 200 to 280 nm) light can be absorbed by DNA, RNA, and proteins[10], and therefore can play a part in viruses' inactivation[11,12]. The radiation of DUV is able to excite two neighbouring thymine molecules in the DNA chain or uracil molecules in RNA of viruses (i.e., break the hydrogen bonds of their original base pairs) and further form a dimer of thymine or uracil, respectively[13]. Sufficient formations of dimers can result in a dysfunction of DNA/RNA replication and thus inactivation of viruses[14], but the lethal effect at the same dose of DUV radiation depends on the viral genetic sequence or proteins[7,15]. Hence, the DUV light disinfection at several wavelengths on different mediums was widely studied and used against the COVID-19 pandemic from the beginning. The DUV dose reported for SARS-CoV-2 inactivation was various from 1.8 to 1048 mJ/cm^2 in literatures[7,9,16–19]. These discrepancies were caused by the inconsistency in wavelengths of the light source, criteria for lethal effect, surface materials and virus infectivity assay, where shorter wavelengths and less viral liquid under light exposure generally required less DUV dose. It is worth noting that current research mainly investigated the DUV disinfection for the original strain (i.e., wildtype, WT), but the variants of Delta and Omicron are also of concern to the World Health Organisation[20]. Meanwhile, the work from Yap et al. (2020) has reported that the average lifetime for SARS-CoV-2 is temperature-dependent, where a longer lifetime at lower temperatures (such as more than one month at 10 °C)[21]. This is the reason why transmission of SARS-CoV-2 on the food cold chain was found[22]. The virucidal efficacy of DUV is also influenced by temperature, such as airborne porcine reproductive and respiratory syndrome virus is more susceptible to ultraviolet as temperature decreased[23], but the influence for SARS-CoV-2 is still unknown.

Therefore, the study presented here conducted experiments regarding DUV light disinfection for SARS-CoV-2 and its variants (Delta and Omicron) at different temperatures, where these variants and the cryogenic environment (such as −20 and −50 °C) were the first to be reported. Simultaneously, the principle behind different disinfection performances was analysed from photoelectronic and photobiological aspects, and the guidance for using DUV to inactivate SARS-CoV-2 in the cryogenic environment was provided.

Materials and methods

DUV light source

The DUV planar light source used in this work was composed of 64-high-power DUV LED chips with centre emission peak at 275 nm (measured by the HAAS-2000 high accuracy array spectroradiometer, EVERFINE) and the chip array was solidified on the copper substrate and attached to a water-cooling plate (made of aluminium material) to ensure the effective heat dissipation and reliable optical power output. The water-cooling system started to work when the temperature over 28 °C. The DUV module was driven by a direct current power supply, and the output optical power was controlled by adjusting the ratio of the current output. The current ratio dependent power density of the DUV light source could be traced in Fig. S1(Supplementary information). In all experiments, the planar light source was fixed at the same height, and the light power intensity in the projection area was measured by an optical power meter (PM100D Power Energy Meter equipped with S120VC sensor head, Thorlabs). Meanwhile, the irradiation time (1 second) was determined by an electronic timer equipped with the drive circuit.

Preparation and inactivation of microorganisms

The *Staphylococcus aureus* (ATCC 6538) used in this study was obtained from the American Type Culture Collection (ATCC) and stored at −80 °C before usage. For ease of use, the bacteria cultures about 1×10^6 colony forming units (CFU) were dropped on the glass slides and dried as biofilms. The Swine-origin influenza A virus (H1N1) was obtained from the Guangdong Institute of Microbiology (Guangzhou, China) with an initial titer of 2×10^5 TCID$_{50}$/mL (the 50% tissue culture infectious dose assay, TCID$_{50}$). The inactivation experiments for ATCC 6538 and H1N1 were conducted according to the Technical Standard for Disinfection (section 2.1.54, Ministry of Health, Edition 2002, China). Before DUV treatments, all samples were stored in the required temperature

conditions (e.g., −50 °C, −40 °C, −20 °C, −18 °C, 5 °C, 23 °C, 37 °C) for at least three hours for temperature stabilisation. Unless otherwise stated, no antifreeze or other reagents were added to the culture medium of all virus and bacteria samples, and this is to keep the situation close to the actual cryogenic environment. After the UV treatment, the bacteria on the glass slides were recovered in tryptic soy broth (TSB) by placing the glass slides in 50 mL centrifuge tubes containing TSB and vortex for 1−2 min. After the recovery of the supernatants and serial dilution, the bacteria were incubated at 37 °C for 24 h on trypticase soy agar (TSA) plates, and the number of colonies forming units was finally calculated. The H1N1 virus was recovered similar as the following SARS-CoV-2 as well as the calculation of $TCID_{50}$ value. The infection and inactivation experiment for SARS-CoV-2 was carried out in biosafety level-3 laboratories (BSLs-3) at Xiamen Center for Disease Control and Prevention (Xiamen, China). All viral strains (WT, Delta (B.1.617.2) and Omicron (BA.1.15)) were propagated in Vero E6 cells, followed by concentration using ultra-high-speed centrifugation and storage at −80 °C before usage according to the protocol of our published work[24]. To determine the disinfection effect of DUV irradiation on SARS-CoV-2, a viral stock solution was prepared at a concentration of 1×10^5 $TCID_{50}$/mL, diluted in ten times, and then irradiated with UV light. DUV exposure was performed of 0.1 mL virus stock in 6-well plates. Before DUV treatments, the samples were all stored in the required temperature conditions (e.g., −50 °C, −20 °C, 23 °C) for at least three hours for temperature stabilisation. The infection of Vero E6 cells was conducted directly after the DUV treatments. Additional 0.9 mL virus maintenance solution containing 10% fetal bovine serum (FBS) and 1% Penicillin/Streptomycin (PS) was added in each well. To ensure the uniformity of irradiation and the accurate dose in the well plate, only one well of each plate is used. Then, the SARS-Cov-2 virus samples were cultured on VERO-E6 cells for 5 days, accompanied with the continuous observation of cell lesions. The $TCID_{50}$ value was finally calculated by Reed-Muench method.

All microorganisms' experiments were carried out in triplicate.

Genetic data and protein information
The gene sequences were gained from the open-source database (National Center for Biotechnology Information, U.S. National Library of Medicine) submitted by the Fudan University (Shanghai, China)[25], as well as the University of Hong Kong (Hong Kong, China)[26]. The untranslated regions of 5'UTR and 3'UTR were removed before the comparison between the WT and Omicron. Besides, the protein information was obtained from the RCSB PDB[27] and further analysed by the ExPASy - ProtParam tool[28] for their physicochemical property.

Temperature data
The temperature data of China was sourced from the National Science & Technology Infrastructure of China[29], and the mean January temperature in 2020 was calculated and used in this study.

Statistical analysis
The data from the inactivation by DUV irradiation were analysed by a multivariate analysis of variance (ANOVA) at an alpha level (α) of 5% with two-way interaction (DUV dose, virus strains, temperatures, and replicates as fixed factors), and significantly different parameters were further analysed with Fisher's least significant difference (LSD) post-hoc test by using XLSTAT (ver. 2016; Addinsoft SARL, Paris, France).

Results and discussion

Construction and verification of the DUV light source
DUV light was emitted from nitride-based LEDs and used for disinfection in this study. These LED chips were fabricated based on our proven technologies in the published work[30], and the optical power of a single chip was able to reach 50 mW that is a high value for the current commercial 260–280 nm LED in the industry. The structure demonstration of the DUV LED chip was shown in Fig. 1(a), and a typical flip-chip structure was applied. Meanwhile, a SiO_2/Al electrode (it has advantages for improving both the extraction of transverse magnetic-polarised light by surface plasmon and the reflection of light)[31] combined with the thin p-GaN layer was used to improve the light output power (LOP). In addition, the UV germicidal effectiveness peaks at around 265 nm corresponding to the peak of UV absorption for DNA/RNA within viruses or bacteria[15,32]. Hence, the central emission wavelength of LEDs was modulated to 275 nm through a design of the quantum well structure with a 10-nm full width at half maximum (Fig. 1(b)), which also took a compromise from wall-plug efficiency (WPE) into consideration. At the same time, the selected
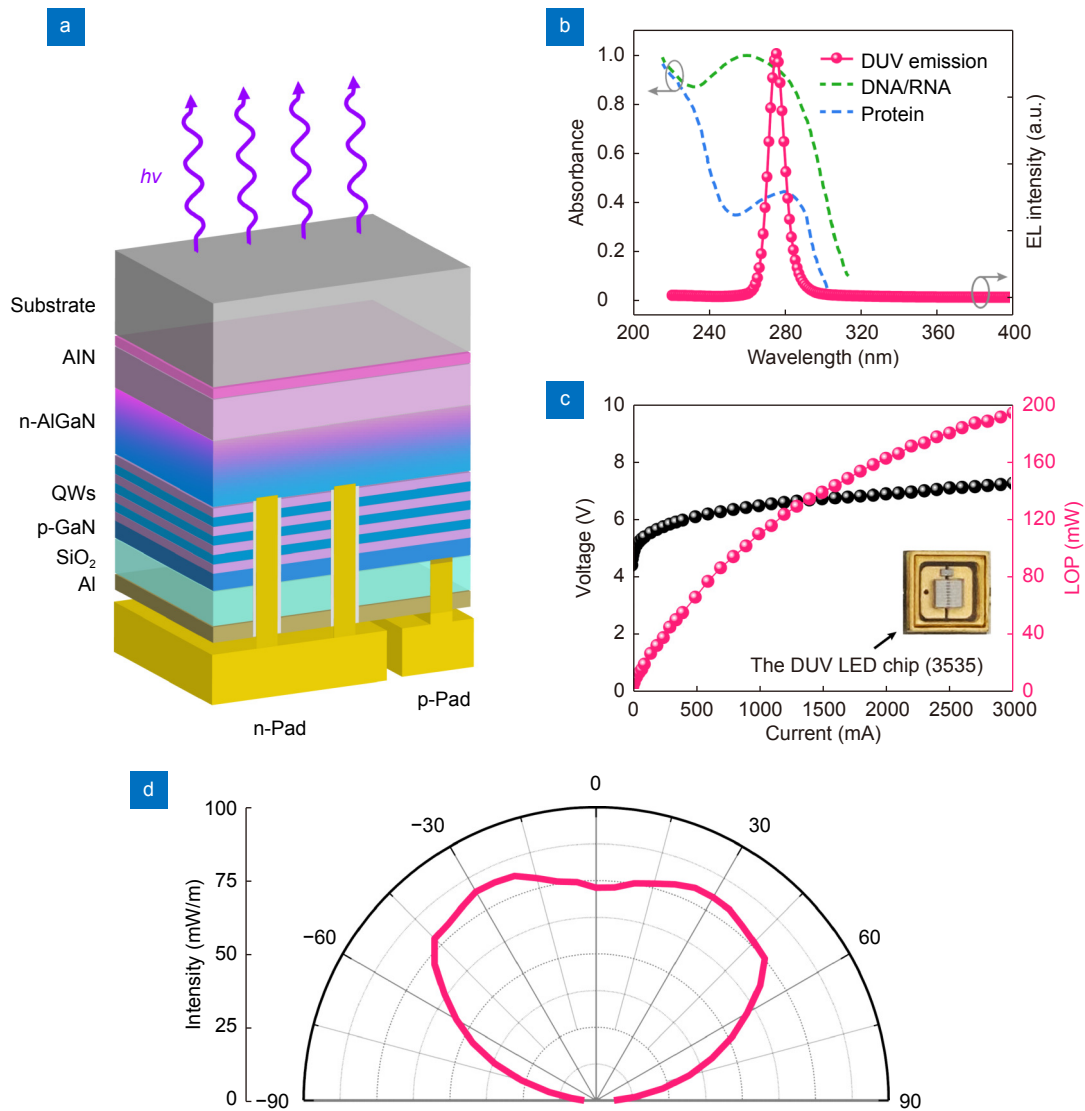
Fig. 1 | The fabricated DUV LED chip. (**a**) Schematic diagram of the LED structure. (**b**) Electroluminescence (EL) spectrum of the fabricated chip. The green and blue dotted lines were the standard absorption spectra of DNA/RNA and proteins extracted from published values, respectively (also known as germicidal effectiveness curve).[15] (**c**) Measured *I-V* and LOP characteristics of the chip. (**d**) Angular emission pattern for the chip.

wavelength was still in the DNA/RNA and protein germicidal absorption region. The measured current-voltage (*I-V*) and LOP characteristics of the chips were displayed in Fig. 1(c). At the driving current of 350 mA, an approximately 50.3 mW LOP was achieved with a WPE of 2.43 % at room temperature. This WPE was close to the values of advanced commercial DUV LED[30]. The angular emission pattern of LED chips was displayed (Fig. 1(d)). The emitted light was distributed across an angle range of approximately 120 and was relatively more uniform and stronger from −45° to 45°. The fabricated LED chips ensured a high optical power, but a light source providing uniform and reliable DUV within a large area is still in need of disinfection. The WPE of

DUV LED is much lower than the visible-light LED at the current stage, majority of energy converts to heat and thus results in a challenge of heat dissipation. Furthermore, it is difficult to enhance the LOP and the radiation area by simply increasing the size of the LED. A LED array with a secondary light distribution design and the water-cooling system could address these difficulties.

Therefore, 64 fabricated chips were further assembled in an 8×8 arrangement with 5-mm intervals, as shown in Fig. 2(a, b). This assembled module could stably emit at least 30 mW/cm² DUV to a projection area with a diameter of 2 cm, and the unevenness was less than 5 % (the distance between light source and projection was 4.5 cm). It was because the disinfection experiments were all
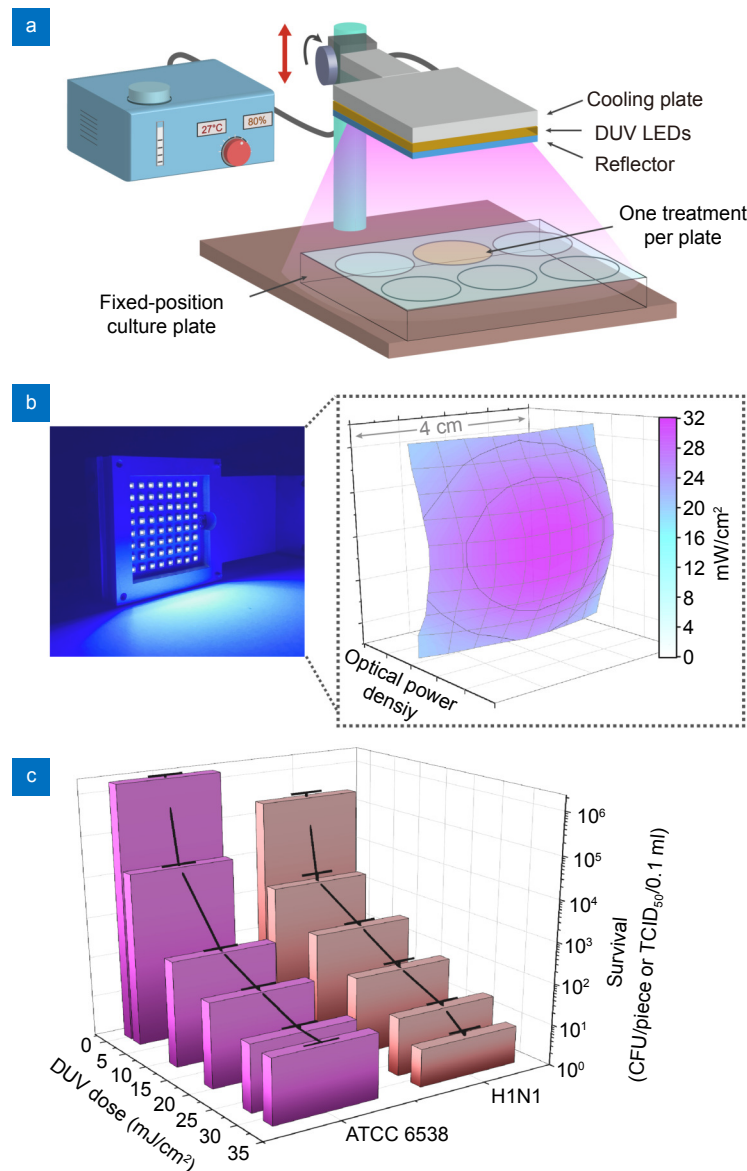
Fig. 2 | The assembled DUV module. (**a**) Schematic diagram of the module. Two monitors were used to show the temperature of the cooling plate and the driving current of the whole module. (**b**) Photo of the module in work (left, where 64 LED chips were inset) and the corresponding optical power density measurement (right, the distance between the light source and projection was 4.5 cm). (**c**) DUV inactivation tests on the ATCC 6538 and H1N1 at 23 °C. CFU and TCID$_{50}$ stood for colony-forming units and 50% tissue culture infectious dose, respectively.

conducted within a 1 cm^2 area, thus uniformity and coverage of this light source met the requirements. Subsequently, the DUV inactivation ability of the assembled module was tested on the ATCC 6538 and H1N1 at 23 °C. These two microorganisms especially the ATCC 6538 are widely used as reference standards/alternatives to evaluate the virucidal efficacy or establish a statistical model in the inactivation experiments, such as mentioned in the Global Lighting Association's guidance (Germicidal UV-C Irradiation: Sources, Products and Applications) and the requirements in the Chinese technical standard GB 28235-2020 (hygienic requirements

for the ultraviolet appliance of disinfection). In our test, one-second irradiation time was fixed and ensured by a digital timer, and DUV doses were modulated (from 1.91 to 31.2 mJ/cm^2) by changing the drive current of the assembled module. The survival of ATCC 6538 and H1N1 was dramatically reduced with the increased DUV dose (Fig. 2(c)), where the 2-log and 4-log reductions were achieved at the dose of approximately 2 and 27 mJ/cm^2, respectively. These DUV radiation doses were corresponding with the published works of literature[33−35], and a typical two-stage inactivation performance was also observed from both ATCC 6538 and H1N1 (i.e., a faster

reduction rate in the first but a relatively slower rate in the second stage)[36,37]. The two different stages of inactivation were due to a high-level resistance against environmental changes in a small portion of microorganism populations, including the increase of DUV. From the observations mentioned above, the high optical power density, good radiation uniformity, and effective biological inactivation capacity of this developed DUV module were confirmed.

Preliminary test for the effect of cryogenic environment on the DUV disinfection

As mentioned in the introduction, the virucidal efficacy of DUV can be influenced by temperature. The effects from the low temperatures (such as 5 °C, −18 °C and −40 °C) were evaluated in the first place on ATCC 6538 and shown in Fig. 3(a–e). The lethal effect of DUV was analysed by a first-order kinetic model following the equation below[37]:

$$\frac{N}{N_0} = (1-f)\,e^{-r_1 D} + f e^{-r_2 D} \,, \qquad (1)$$

where N is the survival count after the irradiation dose of D (mJ/cm²), N_0 is the initial amount, f is UV resistant fraction, and r is the first-order inactivation rate constant (r_1 and r_2 indicate for the first and second stage of

the typical two-stage inactivation performance, respectively). The r_1 and r_2 were changed with the decreasing temperatures, and their variation trends were opposite. The r_1 was doubled and the r_2 was reduced six times when temperature changing from 37 °C to −40 °C. Notably, the r_2 was relatively more important for the bacterial saturated elimination (reflected by those microorganism populations having a high-level resistance against environmental changes). The r_2 was further involved in the model based on the Arrhenius equation[38,39], because the mechanism of DUV affecting on the genetic material is a typical physicochemical reaction[40,41]:

$$\ln(r_2) = -\frac{E_A}{R_c T(K)} + \ln(A) \,, \qquad (2)$$

where E_A is the Arrhenius activation energy for inactivation of the microorganism, $T(K)$ is the absolute temperature, R_c is the universal gas constant, and A is the constant frequency factor. The fitting model of the DUV virucidal efficacy for ATCC 6538 under different environment temperatures was therefore obtained and simultaneously shown in Fig. 3(f). Certainly, the impact of temperature on the DUV disinfection would slightly differ by the specific disinfection object, and there might be a difference between the ATCC 6538 and the SARS-CoV-2 requiring an experimental verification.
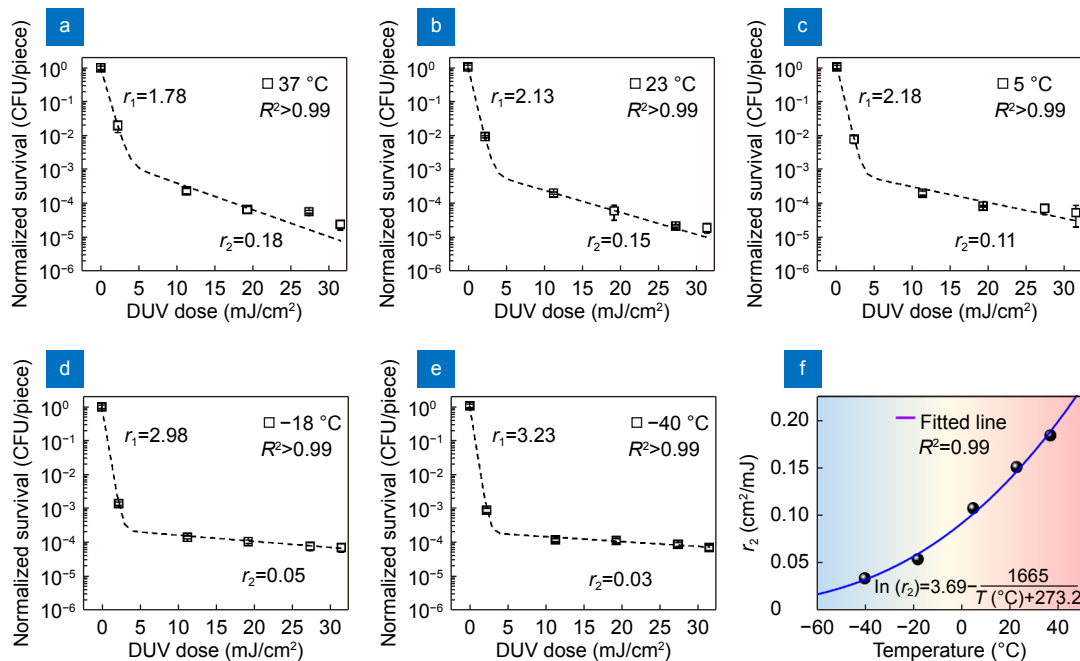

Fig. 3 | DUV disinfection on the ATCC 6538. (**a-e**) DUV virucidal efficacy at five experimental temperatures. The *r* is the first-order inactivation rate constant, and r_1 and r_2 indicate for the first and second stage of the typical two-stage inactivation performance, respectively. (**f**) Fitting model of the DUV virucidal efficacy under different environment temperatures based on the Arrhenius equation. *T*(°C) is the temperature in degrees centigrade.

DUV disinfection on SARS-CoV-2 and its variants at different temperatures

The DUV module was subsequently applied to the SARS-CoV-2 (including the strains of WT, Delta and Omicron) at three different temperatures (23 °C, −20 °C, and −50 °C) to investigate the lethal effect evaluating by the $TCID_{50}$ assay. The SARS-CoV-2 inactivation data were presented in Fig. S2, and an initial exploration of data (the reduction of $TCID_{50}$) was carried out through a multivariate ANOVA, shown in Table 1 and Fig. S3. The experimental repeatability was firstly checked, and there was no significant difference between replicates. Meanwhile, the virucidal efficacy was significantly influenced by the factors of DUV dose, temperature, and viral strain as well as their interactions (all p values were ≤ 0.05). For ease of interpretation, the data were visualised separately in Fig. 4. The effects from factors of DUV dose and temperature were presented by a heat map (Fig. 4(a)), which provisionally ignored the difference between the strains and considered them as SARS-CoV-2 merely. It was clear to see that the inactivation of SARS-CoV-2 was positively and significantly related to the temperatures and DUV doses, and it was similar to the findings from previous literature conducting UV inactivation experiment of other microorganisms at different temperatures[42]. The virucidal efficacy of DUV light for SARS-CoV-2 was significantly differentiated at −50 °C, and the dose of 26.6 mJ/cm² was close to the saturation of inactivation at every temperature. But remarkably, the Omicron differed from other strains significantly, and the discrepancies were illustrated by response surfaces in detail (Fig. 4(b)). This variant seems to have a higher tolerance against DUV light compared to the WT and Delta, and the irradiation of 31.2 mJ/cm² at 23 °C did not result in its complete deactivation. Furthermore, the DUV disinfection on the Omicron was more temperature-dependent, where the virucidal efficacy was approx-

imately suppressed a half by the −50 °C environment. Therefore, these notable phenomena from the cryogenic environment and the Omicron should be further studied to understand the principle behind different disinfection performances.

Elucidation of the discrepancies caused by the temperature and viral strain

Firstly, the impact of temperature on DUV disinfection was theoretically analysed from the photoelectronic aspect, and the interpretation was displayed by using configuration coordinates (Fig. 5). Figure 5(a, b) showed the transition of electrons within the active genetic molecules inducing by a photon or temperature. Thanks to this transition, those electrons were able to conduct a relaxation and overcame the barrier, and further resulted in physicochemical reactions (such as the covalent bond formation of the cyclobutane pyrimidine dimers (CPDs) or the cross-linking between pyrimidine and proteins)[43,44]. Furthermore, the DUV disinfection was a continuous process involving multiple photons, and products from the physicochemical reactions were more stable on energy (because the formed covalent bond is significantly more stable than the initial hydrogen bonding)[45]. At the same time, the energy of the barrier would increase for the subsequent reactions when more physicochemical reactions happened. Hence, the final energy state and barrier in the configuration coordinates would continuously change due to the accumulation of those reactions, and the negative-U large-relaxation model could be used to demonstrate the DUV disinfection process (Fig. 5(c)). The comparison between low- and high- temperature situations (the low or high here was a relative term) was displayed in Fig. 5(d). Low- or high- temperature situations provided different thermal energy and thus resulted in different initial photo-ionised positions before the DUV irradiation. Therefore, the electrons within the

Table 1 | Multivariate ANOVA of SARS-CoV-2 inactivation by DUV irradiation with two-way interaction.

	Degree of freedom	*F*	§*p*
Replicate	2	0.567	0.5690
DUV dose	5	505.024	**< 0.0001**
Temperature	2	5.749	**0.0040**
Viral strain	2	342.607	**< 0.0001**
DUV dose*Temperature	10	2.499	**0.0100**
DUV dose*Viral strain	10	25.285	**< 0.0001**
Temperature*Viral strain	4	15.949	**< 0.0001**

§ Bold *p* values represent the significant differences at an alpha level of 5%.
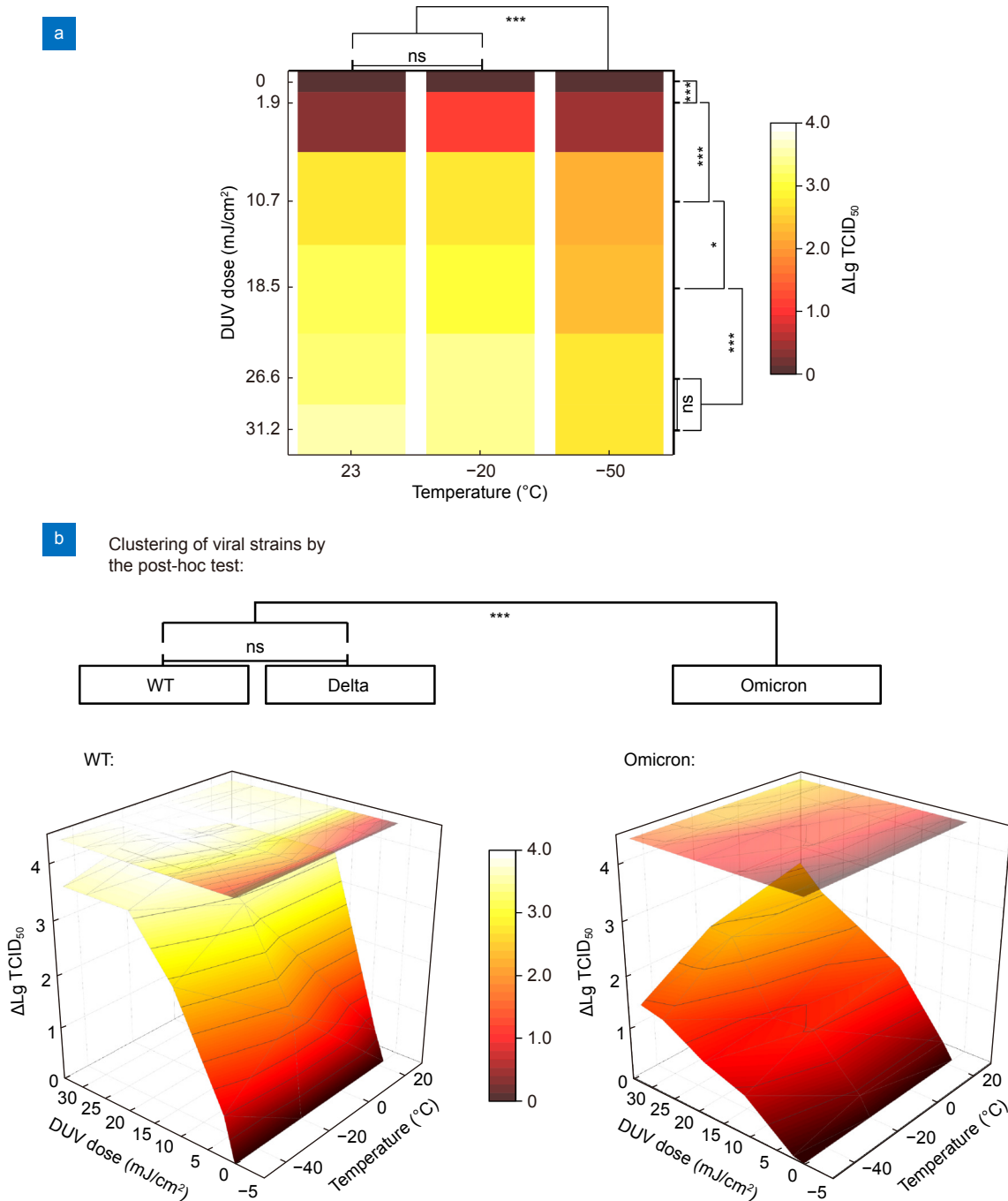
Fig. 4 | DUV disinfection on SARS-CoV-2 and its variants. Symbols *, **, and *** denoted for *p* value < 0.05, 0.01, and 0.001 respectively from the multivariate ANOVA analyses, and the results of Fisher's least significant difference (LSD) post-hoc test were simultaneously indicated by the clustering. (**a**) SARS-CoV-2 inactivation changing with the coeffects between different temperatures and DUV doses. (**b**) Difference between viral strains and their response surfaces of DUV inactivation.

active genetic molecules residing at a higher temperature were easier to be excited by the same DUV dose and had more opportunity to overcome the barrier. As consequent, the accumulation phenomena in the high-temperature situation would be relatively more obvious than that in the low-temperature situation, expressing as the final state S_2 was lower than S_1 and the relaxation dis-

tance between L_2 and L_0 was longer. Finally, the chance of capture back to the initial state C_2 would be much lower than C_1. Based on the reasons mentioned, the lethal effect of DUV irradiation would be higher in a higher temperature situation.

Secondly, the effect of the variant Omicron on DUV disinfection was analysed. There were two possibilities,
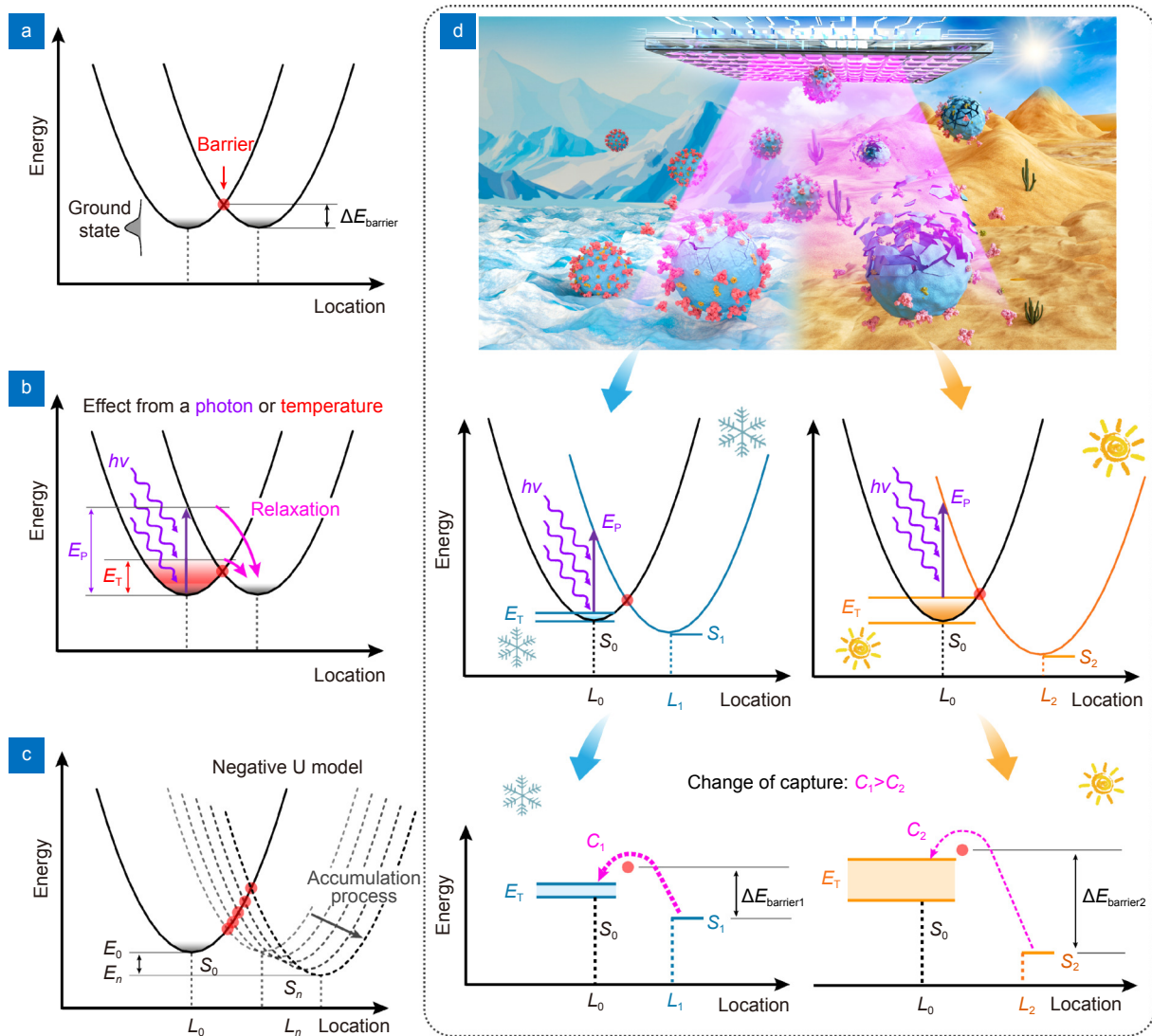
Fig. 5 | Influence of temperature on the DUV disinfection. (**a**) Configuration coordinate for situation without the effect from photon and temperature. $\Delta E_{barrier}$ was the energy difference between the barrier and the energy states. (**b**) The electroacoustic coupling process in which electrons in genetic material (DNA or RNA) being affected by a photon or temperature. E_T and E_P represented thermal and photonic energy, respectively. (**c**) The accumulation process induced by the electroacoustic coupling, in which the negative U model was involved. S_0 and S_n stood for the state before disinfection and the state after disinfection, respectively. (**d**) The influence of low- (left) and high-temperature (right) on the DUV disinfection. S_0, S_1, and S_2 stood for the ground state and two final states, respectively. C_1 and C_2 were the chances of capture.

gene sequence and protein composition, to make the Omicron significantly differ from other strains. As shown in Fig. 6(a), the inactivation of (+) single-stranded RNA viruses were mainly caused by the formation of UU (uracil/uracil) and UC (uracil/cytosine) dimers after the UV radiation. The published literature has demonstrated that these formed CPDs were relatively stable and required much higher excitation energy to initiate the photo-reversibility process back to their original monomer pyrimidines[45]. The possibility of dimers formation was related to the number of Cs, Us, UUs, and UUUs in the gene sequence[46]. The WT had more num-

bers on Cs (5761 vs. 5755), Us (8794 vs. 8792), and UUs (2124 vs. 2122) but fewer UUUs (636 vs. 640) than the Omicron according to the known genetic data (NC_045512.2 and ON600286.1)[25,26]. Therefore, the UV-induced inactivation possibility of WT was slightly higher from the aspect of the gene sequence. In addition, the proteins, another factor but could be more important contributing to the discrepancies of the Omicron. The proteins could affect the final DUV intensity radiated on the viral RNA chains (Fig. 6(b)). A comparison for the spike (S) proteins was conducted between the WT and Omicron (Table S1), and we found the Omicron had a
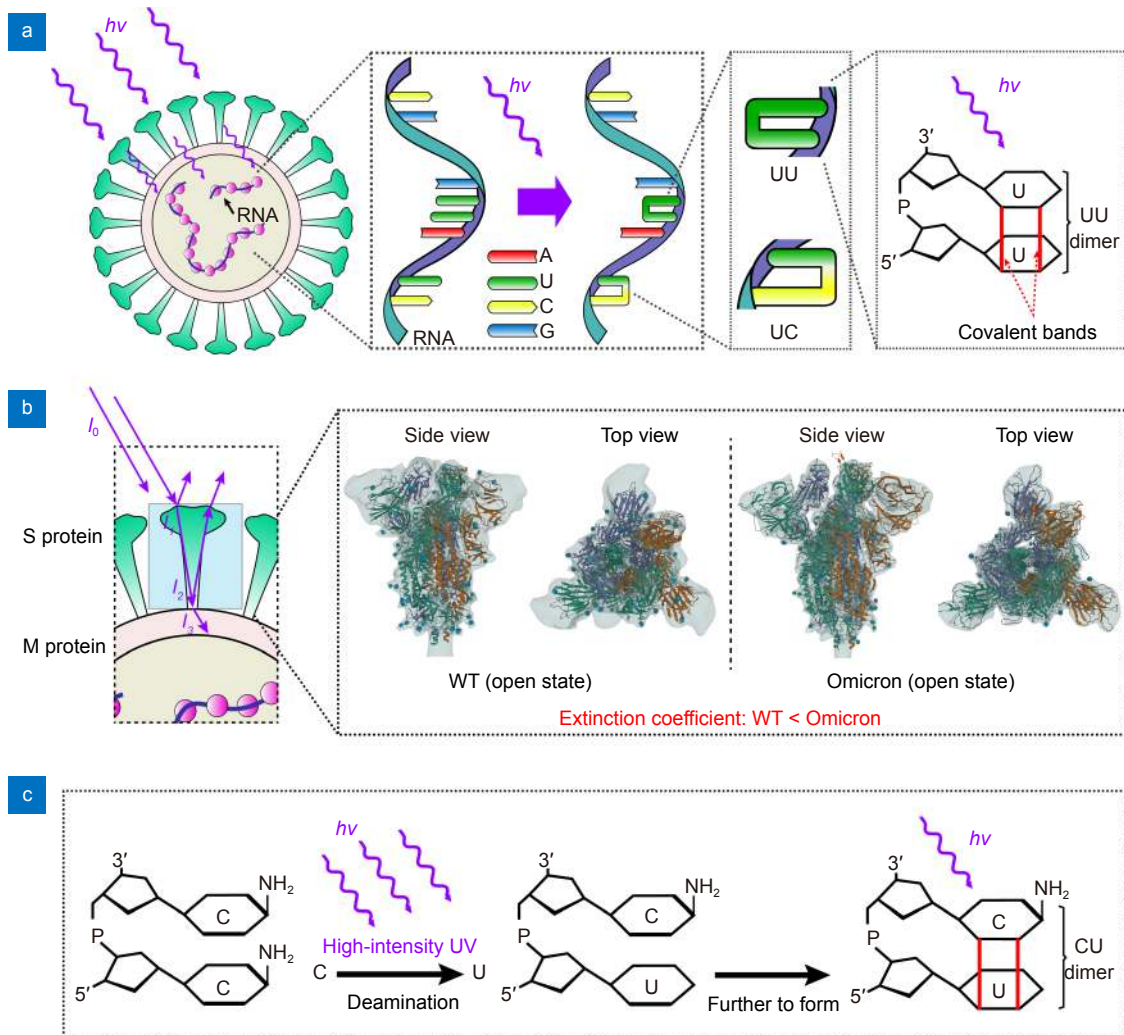
Fig. 6 | Influence from the variant Omicron on DUV disinfection. (**a**) The aspect of the gene sequence. (**b**) The aspect of proteins. I_0 to I_3 represented the intensities of DUV from the initial state passing through the S proteins and getting into the M proteins, respectively. The abbreviation of S and M stood for spike and membrane proteins. (**c**) The possible photochemical changes by the high-intensity UV (the DUV-induced gene mutations).

higher extinction coefficient (k) in both open and close states. The k is positively related to the absorption and reflectivity[47], and the intensity of DUV would be reduced following the equation below (the detailed derivation procedure was shown in Fig. S4):

$$I_3 = I_0(1-R)^2\exp\left(\frac{-2\omega dk}{c}\right), \qquad (3)$$

where I_0 is the initial DUV intensity, I_3 is the DUV intensity getting into the membrane (M) protein, R is the reflected part of the light, ω is the angular frequency of light, d is the equivalent thickness of the S protein, and c is the speed of light in a vacuum. This indicated that a potentially and relatively lower intensity of DUV would radiate on the RNA chains of Omicron compared to the WT. Lower DUV intensity would directly result in a less CPDs formed from the original bases on the RNA

chains. Meanwhile, the DUV intensity could also influence the chance of CPDs formation from the DUV-induced gene mutations[43,48] (one of two adjacent Cs were deaminated and changed to U, and subsequently from the UC dimers, shown as Fig. 6(c)). Lower intensity of DUV radiating on the RNA chains of Omicron compared to the WT, also meant a less possibility of the DUV-induced gene mutations. Certainly, other proteins could also influence the DUV virucidal efficacy, such as those RNA replication-related non-structural proteins (NSPs)[49], but the limited research available was not enough to support a comparison. Our hypotheses from the gene sequence and S proteins could theoretically explain the differences from Omicron, and further experimental verification is needed in the future.
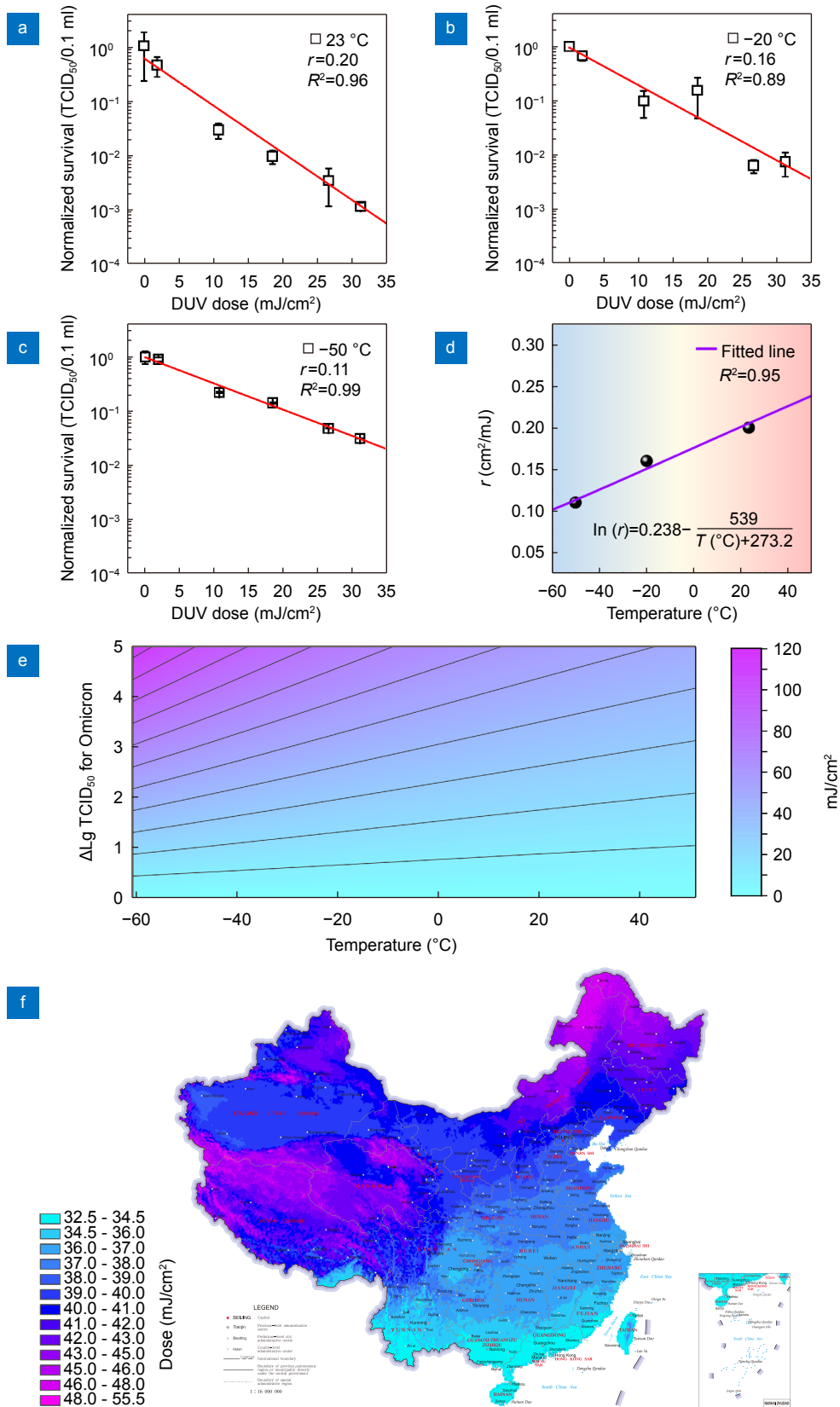
Fig. 7 | DUV disinfection suggestion against the SARS-CoV-2. (**a–c**) DUV virucidal efficacy for Omicron at three experimental temperatures. (**d**) Fitting model of the DUV virucidal efficacy for Omicron under different environment temperatures based on the Arrhenius equation. (**e**) DUV dose required to achieve different lethality at different temperatures. (**f**) DUV dose forecast for obtaining a 3-log reduction of the Omicron in Chinese winter (according to the Mean January temperature).

Suggestion of DUV disinfection against the SARS-CoV-2

Based on the findings above, suggestion of DUV disinfection was made aiming to effectually prevent the disease transmission of COVID-19. This suggestion was developed with a view to the effects of both Omicron and cryogenic conditions, because the virucidal efficacy of DUV light was significantly influenced by these two factors. Firstly, the DUV virucidal efficacy for Omicron at three experimental temperatures were displayed, and as shown in Fig. 7(a–c), classic one-stage inactivation performances were observed. This one-stage performance was different from our ATCC6538 results but in good agreement with published literature working on airborne human coronaviruses (including SARS-CoV-2, alpha HCoV-229E, and beta HCoV-OC43)[50,51]. The one-stage inactivation fitting model was applied to our Omicron inactivation results following the equation below[37]:

$$\frac{N}{N_0} = \mathrm{e}^{-rD} \ . \tag{4}$$

The Omicron activity decreased linearly in logarithms as a function of the DUV dose, meanwhile, the *r* was different at 23 °C, −20 °C, and −50 °C, where 0.20, 0.16, and 0.11 were gained respectively. Subsequently, the Arrhenius equation (Eq. (2)) was also involved (Fig. 7(d)), and the fitting model of the DUV virucidal efficacy for Omicron under different environment temperatures was obtained:

$$\ln(r) = 0.238 - \frac{539}{T\,(°C) + 273.2} \ , \tag{5}$$

where *T*(°C) is the temperature in degrees centigrade. Then, this Eq. (5) was further used to show the DUV dose required for different lethality at different temperatures (Fig. 7(e)). It would be useful to provide guidance for those people or organisations (such as hospitals and customs offices) using DUV to disinfect the SARS-CoV-2. In particular, the suggestion of DUV disinfection in cold conditions (such as food cold chain logistics) is the first to be reported. In addition, China has a vast territory with huge temperature differences in winter, sub-zero temperatures are normal in winter for the north part and the plateau section of China. Thus, these areas require a higher DUV dose to achieve the same virucidal efficacy if the DUV disinfection is used in the open air. A DUV dose forecast for obtaining a 3-log reduction (99.9%) of the Omicron was made in Fig. 7(f), where the 3-log reduction is the requirement in the Chinese technical standard GB 28235-2020 (hygienic requirements for the ultraviolet appliance of disinfection). Based on the observations from the current study, future work could be expanded to investigate other factors, such as roughness of surface or size of nanoparticles[52], for the DUV disinfection of SARS-CoV-2. Furthermore, new types of light source with higher quantum efficiency could be applied in the future, e.g., high density GaN/AlN quantum dots[53] or directional high-efficiency nanowire LEDs[54].

Conclusions

This study demonstrated an effective and fast (in 1 sec) inactivation capacity of the DUV light on SARS-CoV-2 and other microorganisms, meanwhile, the DUV LED module had the advantage to realise a narrow-band DUV emission and uniform radiation (the unevenness was less than 5% on the inactivation surface) reliably. The research gaps regarding the influences of viral variants (Delta and Omicron) and low temperatures on the DUV virucidal efficacy were filled. The lethal effect of DUV was reduced by the cryogenic environment, for instance, the DUV dose needed to be doubled at −50 °C to achieve the same inactivation performance compared to the room temperature for the variant of Omicron. This was mainly elicited by the different thermal energy and chance of capture in the negative-U large-relaxation model. Besides, the inactivation of Omicron required a significantly higher DUV dose compared to other viral strains, which was theoretically due to its genetic and proteinic characteristics. The crucial discoveries in this study can offer human society guidance of DUV disinfection to fight against the COVID-19, especially in the cryogenic conditions (such as the food cold chain logistics and the open air in winter).

References

1. Guan WJ, Ni ZY, Hu Y, Liang WH, Ou CQ et al. Clinical characteristics of coronavirus disease 2019 in China. *N Engl J Med* **382**, 1708–1720 (2020).
2. Douglas M, Katikireddi SV, Taulbut M, McKee M, McCartney G. Mitigating the wider health effects of covid-19 pandemic response. *BMJ* **369**, m1557 (2020).
3. Tian DD, Sun YH, Zhou JM, Ye Q. The global epidemic of the SARS-CoV-2 delta variant, key spike mutations and immune escape. *Front Immunol* **12**, 751778 (2021).
4. Karim SSA, Karim QA. Omicron SARS-CoV-2 variant: a new chapter in the COVID-19 pandemic. *Lancet* **398**, 2126–2128 (2021).
5. Douaud G, Lee S, Alfaro-Almagro F, Arthofer C, Wang CY et al.

SARS-CoV-2 is associated with changes in brain structure in UK Biobank. *Nature* **604**, 697–707 (2022).

6. Goswami N, He YR, Deng YH, Oh C, Sobh N et al. Label-free SARS-CoV-2 detection and classification using phase imaging with computational specificity. *Light Sci Appl* **10**, 176 (2021).

7. Raeiszadeh M, Adeli B. A critical review on ultraviolet disinfection systems against COVID-19 outbreak: applicability, validation, and safety considerations. *ACS Photonics* **7**, 2941–2951 (2020).

8. Berry G, Parsons A, Morgan M, Rickert J, Cho H. A review of methods to reduce the probability of the airborne spread of COVID-19 in ventilation systems and enclosed spaces. *Environ Res* **203**, 111765 (2022).

9. Bormann M, Alt M, Schipper L, van de Sand L, Otte M et al. Disinfection of SARS-CoV-2 contaminated surfaces of personal items with UVC-LED disinfection boxes. *Viruses* **13**, 598 (2021).

10. Gray NF. Ultraviolet disinfection. In Percival SL, Yates MV, Williams DW, Chalmers RM, Gray RNF. *Microbiology of Waterborne Diseases* 617–630 (Elsevier, Amsterdam, 2014).

11. Aoyagi Y, Takeuchi M, Yoshida K, Kurouchi M, Yasui N et al. Inactivation of bacterial viruses in water using deep ultraviolet semiconductor light-emitting diode. *J Environ Eng* **137**, 1215–1218 (2011).

12. Minamikawa T, Koma T, Suzuki A, Nagamatsu K, Yasui T et al. Inactivation of SARS-CoV-2 by deep ultraviolet light emitting diode: a review. *Jpn J Appl Phys* **60**, 090501 (2021).

13. Bolton J, Cotton C. Mechanism of UV disinfection. In Bolton JR, Cotton CA. *The Ultraviolet Disinfection Handbook* (American Water Works Association, Denver, 2008).

14. Oguma K, Katayama H, Ohgaki S. Photoreactivation of *Escherichia coli* after low- or medium-pressure UV disinfection determined by an endonuclease sensitive site assay. *Appl Environ Microbiol* **68**, 6029–6035 (2002).

15. Sharma VK, Demir HV. Bright future of deep-ultraviolet photonics: emerging UVC chip-scale light-source technology platforms, benchmarking, challenges, and outlook for UV disinfection. *ACS Photonics* **9**, 1513–1521 (2022).

16. Heilingloh CS, Aufderhorst UW, Schipper L, Dittmer U, Witzke O et al. Susceptibility of SARS-CoV-2 to UV irradiation. *Am J Infect Control* **48**, 1273–1275 (2020).

17. Biasin M, Bianco A, Pareschi G, Cavalleri A, Cavatorta C et al. UV-C irradiation is highly effective in inactivating SARS-CoV-2 replication. *Sci Rep* **11**, 6260 (2021).

18. Liu SF, Luo W, Li D, Yuan Y, Tong W et al. Sec‑eliminating the SARS‑CoV‑2 by AlGaN based high power deep ultraviolet light source. *Adv Funct Mater* **31**, 2008452 (2021).

19. Sabino CP, Sellera FP, Sales-Medina DF, Machado RRG, Durigon EL et al. UV-C (254 nm) lethal doses for SARS-CoV-2. *Photodiagnosis Photodyn Ther* **32**, 101995 (2020).

20. Variant of Concern. https://www.cdc.gov/coronavirus/2019-ncov/variants/variant-classifications.html#concern (2021), [cited, 2022].

21. Yap TF, Liu Z, Shveda RA, Preston DJ. A predictive model of the temperature-dependent inactivation of coronaviruses. *Appl Phys Lett* **117**, 060601 (2020).

22. Chi YH, Wang QX, Chen GS, Zheng SL. The long-term presence of SARS-CoV-2 on cold-chain food packaging surfaces indicates a new COVID-19 winter outbreak: a mini review. *Front Public Health* **9**, 650493 (2021).

23. Cutler TD, Wang C, Hoff SJ, Zimmerman JJ. Effect of temperature and relative humidity on ultraviolet (UV$_{254}$) inactivation of airborne porcine respiratory and reproductive syndrome virus. *Vet Microbiol* **159**, 47–52 (2012).

24. Su JY, Zheng J, Huang W, Zhang YL, Lv CR et al. PIKfyve inhibitors against SARS-CoV-2 and its variants including Omicron. *Sig Transduct Target Ther* **7**, 167 (2022).

25. Wu F, Zhao S, Yu B, Chen YM, Wang W et al. A new coronavirus associated with human respiratory disease in China. *Nature* **579**, 265–269 (2020).

26. To KW, Yuen KY. Severe acute respiratory syndrome coronavirus 2 isolate SARS-CoV-2/human/HKG/HKU-220213-257/2021, complete genome. https://www.ncbi.nlm.nih.gov/nuccore/ON600286.1 (25-May-2022), [cited, 2022].

27. RCSB PDB. https://www.rcsb.org/ (2022), [cited, 2022].

28. ExPASy – ProtParam tool. https://web.expasy.org/protparam/ (2022), [cited, 2022].

29. 1 km monthly temperature and precipitation dataset for China. http://www.geodata.cn/data/datadetails.html?dataguid=164304785536614&docId=490 (2021-04-23, 2021), [cited, 2022].

30. Li JC, Gao N, Cai DJ, Lin W, Huang K et al. Multiple fields manipulation on nitride material structures in ultraviolet light-emitting diodes. *Light Sci Appl* **10**, 129 (2021).

31. Zhong ZB, Zheng XL, Li JC, Zheng JJ, Zang YS et al. Fabrication of high-voltage flip chip deep ultraviolet light-emitting diodes using an inclined sidewalls structure. *Phys Status Solidi A* **216**, 1900059 (2019).

32. Gerchman Y, Mamane H, Friedman N, Mandelboim M. UV-LED disinfection of coronavirus: wavelength effect. *J Photochem Photobiol B:Biol* **212**, 112044 (2020).

33. Kojima M, Mawatari K, Emoto T, Nishisaka-Nonaka R, Bui TKN et al. Irradiation by a combination of different peak-wavelength ultraviolet-light emitting diodes enhances the inactivation of influenza a viruses. *Microorganisms* **8**, 1014 (2020).

34. Krishnamurthy K, Demirci A, Irudayaraj J. Inactivation of *Staphylococcus aureus* by pulsed UV-light sterilization. *J Food Prot* **67**, 1027–1030 (2004).

35. Krishnamurthy K, Demirci A, Irudayaraj JM. Inactivation of *Staphylococcus aureus* in milk using flow-through pulsed UV-light treatment system. *J Food Sci* **72**, M233–M239 (2007).

36. Kaplan C. The heat inactivation of vaccinia virus. *J Gen Microbiol* **18**, 58–63 (1958).

37. Kowalski W. *Ultraviolet Germicidal Irradiation Handbook: UVGI for Air and Surface Disinfection* (Springer, Berlin, 2009); https://doi.org/10.1007/978-3-642-01999-9.

38. Dewey WC. Arrhenius relationships from the molecule and cell to the clinic. *Int J Hyperthermia* **10**, 457–483 (1994).

39. Becskei A, Rahaman S. The life and death of RNA across temperatures. *Comput Struct Biotechnol J* **20**, 4325–4336 (2022).

40. Song L, Farrah SR, Baney RH. Bacterial inactivation kinetics of dialdehyde starch aqueous suspension. *Polymers* **3**, 1902–1910 (2011).

41. Cebrián G, Condón S, Mañas P. Physiology of the inactivation of vegetative bacteria by thermal treatments: mode of action, influence of environmental factors and inactivation kinetics. *Foods* **6**, 107 (2017).

42. Severin BF, Suidan MT, Engelbrecht RS. Effect of temperature on ultraviolet light disinfection. *Environ Sci Technol* **17**, 717–721 (1983).

43. Sadraeian M, Zhang L, Aavani F, Biazar E, Jin DY. Viral inactivation by light. *eLight* **2**, 18 (2022).

44. Li SS, Paulsson M, Björn LO. Temperature-dependent formation and photorepair of DNA damage induced by UV-B radiation in suspension-cultured tobacco cells. *J Photochem Photobiol B:Biol* **66**, 67–72 (2002).

45. González-Ramírez I, Roca-Sanjuán D, Climent T, Serrano-Pérez JJ, Merchán M et al. On the photoproduction of DNA/RNA cyclobutane pyrimidine dimers. *Theor Chem Acc* **128**, 705–711 (2011).

46. Rockey NC, Henderson JB, Chin K, Raskin L, Wigginton KR. Predictive modeling of virus inactivation by UV. *Environ Sci Technol* **55**, 3322–3332 (2021).

47. Kartalopoulos SV. *Introduction to DWDM Technology: Data in A Rainbow* (Wiley-IEEE Press, Piscataway, NJ, USA, 1999).

48. Barak Y, Cohen-Fix O, Livneh Z. Deamination of cytosine-containing pyrimidine photodimers in UV-irradiated DNA. Significance for UV light mutagenesis. *J Biol Chem* **270**, 24174–24179 (1995).

49. Ricciardi S, Guarino AM, Giaquinto L, Polishchuk EV, Santoro M et al. The role of NSP6 in the biogenesis of the SARS-CoV-2 replication organelle. *Nature* **606**, 761–768 (2022).

50. Minamikawa T, Koma T, Suzuki A, Mizuno T, Nagamatsu K et al. Quantitative evaluation of SARS-CoV-2 inactivation using a deep ultraviolet light-emitting diode. *Sci Rep* **11**, 5070 (2021).

51. Buonanno M, Welch D, Shuryak I, Brenner DJ. Far-UVC light (222 nm) efficiently and safely inactivates airborne human coronaviruses. *Sci Rep* **10**, 10285 (2020).

52. Chen LW, Hong MH. Functional nonlinear optical nanoparticles synthesized by laser ablation. *Opto-Electron Sci* **1**, 210007 (2022).

53. Yang WH, Li JC, Zhang Y, Huang PK, Lu TC et al. High density GaN/AlN quantum dots for deep UV LED with high quantum efficiency and temperature stability. *Sci Rep* **4**, 5166 (2014).

54. Qian YZ, Yang ZY, Huang YH, Lin KH, Wu ST. Directional high-efficiency nanowire LEDs with reduced angular color shift for AR and VR displays. *Opto-Electron Sci* **1**, 220021 (2022).

Acknowledgements

Author contributions

W. Y. Kang, J. Yin, and J. Y. Kang conceived the concept, fabricated the devices, and conducted the characterization of the devices. J. Zheng and L. N. Jiang carried out the SARS-CoV-2 experiments. W. Y. Kang and J. Yin took charge of other experiments, provided all data analysation and presentations, and drafted the manuscript. All the authors discussed the results and contributed to the writing of the manuscript. J. Y. Kang and Y. Wang took charge of supervision.

Competing interests

Supplementary information

The current dependent power density of the DUV light source, the SARS-CoV-2 inactivation data and partial data exploration, the comparison for the spike proteins between the WT and Omicron, and the detailed derivation procedure of the equation (3) could be found in the Supplementary information.
https://doi.org/10.29026/oea.2023.220201